

Passively Mode-Locked High-Power (210 mW) Semiconductor Lasers at 1.55- μm Wavelength

Faisal R. Ahmad and Farhan Rana, *Member, IEEE*

Abstract—We report on the generation of stable passively mode-locked pulses at 1.55- μm wavelength from high-power electrically pumped, large transverse mode semiconductor diode lasers. Optical pulses as short as 5.8 ps were measured directly from the laser. This is the shortest pulsewidth reported (without external compression) from a monolithic mode-locked slab coupled optical waveguide laser. The highest average power measured in mode-locked operation was 212 mW albeit the pulsewidths were larger. It was also found that length of the laser changes the power-current efficiency with the largest recorded efficiency of 165 mW/A.

Index Terms—Mode-locking, quantum-well-based semiconductor lasers.

I. INTRODUCTION

THERE HAS been a growing interest in high-power, electrically pumped mode-locked lasers [1], [2]. These devices have great utility as compact low noise sources for photonic analog-to-digital conversion, radio-frequency (RF) frequency generation, and long-haul high-data-rate optical communication systems [3], [4]. Higher pulse energies also aid in reducing both pulse timing and frequency noise, as these scale inversely with the pulse photon number [5]. Conventional semiconductor mode-locked lasers, although compact and in many cases more economical compared to their solid-state and fiber laser counterparts, produce pulse energies that are typically less than a few picojoules. Various schemes have been employed to generate high energy pulses from semiconductor lasers by increasing the effective mode area; these included multi-element laser arrays, bowtie-shaped gain regions, and optically pumped vertical-external-cavity surface-emitting lasers [6]–[8]. Higher pulse energies can be obtained by increasing the gain saturation energy, which is given by the following expression: [9]

$$E_{\text{sat}} = \frac{\hbar\omega A_{\text{eff}}}{dg/dN}. \quad (1)$$

Here, $\hbar\omega$ is the photon energy, A_{eff} is the effective mode area, and dg/dN is the differential gain. Since E_{sat} is directly proportional to $A_{\text{eff}} = A/\Gamma$, where A is the active region area and Γ is the gain confinement factor, higher pulse energies are

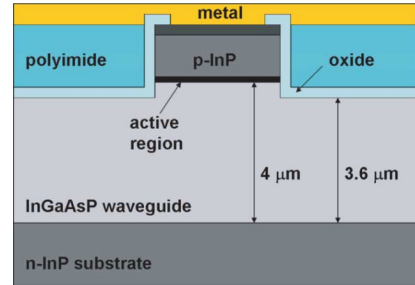


Fig. 1. Schematic of the cross section of the laser. The mode resides mainly in the InGaAsP waveguide layer.

possible by increasing A and decreasing Γ . Typical saturation energies are around 1–2 pJ for $A_{\text{eff}} \approx 1 \mu\text{m}^2$ and assuming $dg/dN \approx 7 \times 10^{-16} \text{ cm}^2$.

Recently, passive mode-locking in an electrically pumped slab-coupled optical waveguide laser has been demonstrated at 1.55 μm [10]. These lasers produced pulse energies as large as 58 pJ. The slab-coupled optical waveguide geometry offers an attractive option for generating high pulse energies because the waveguide structure results in more than an order of magnitude reduction in the gain confinement factor compared to traditional edge-emitting lasers [11], [12]. Hence, the gain saturation energies in these lasers can reach several tens of picojoules.

In this letter, we demonstrate the generation of pulses as short as 5.8 ps from a slab-coupled optical waveguide laser structure. This is the shortest pulsewidth generated from a high-power slab-coupled optical waveguide-based monolithic mode-locked laser without the aid of external compression techniques. We also report power-current efficiency as large as 165 mW/A.

II. FABRICATION AND EXPERIMENT

The multiple-quantum-well structure (shown in Fig. 1) for our laser was grown via metal-organic vapor phase epitaxy on an n-type InP substrate. The mode guiding layer is a 4- μm InGaAsP slab ($\lambda_g = 1.04 \mu\text{m}$) which is lightly doped ($n = 6.5 \times 10^{16} \text{ cm}^{-3}$). This is followed by a 115-nm-thick active region which consists of five periods of InGaAsP quantum wells and barriers. The thickness of the quantum wells and barriers ($\lambda_g = 1.25 \mu\text{m}$) are 8 and 10 nm, respectively. The active region is followed by a 1.1- μm graded doped p-type InP cladding ($p = 0.2 - 1 \times 10^{18} \text{ cm}^{-3}$). The top contact layer is a heavily p⁺-doped 0.2- μm InGaAs layer. The gain confinement factor for the above-mentioned epitaxial structure with a ridge width and height of 4.5 and 1.9 μm , respectively, was calculated to be 0.01, which is three times larger compared to the laser reported by Plant *et al.* [10]. The larger gain confinement factor was chosen to reduce the threshold current and also reduce the cavity length in order to achieve a higher repetition rate. The

Manuscript received August 1, 2007; revised October 4, 2007. This work was supported by National Science Foundation (NSF) Career Grant 0348501, by NSF Grant 0334986, and by Infotonics Inc.

F. R. Ahmad is with the Department of Physics, Cornell University, Ithaca, NY 14853 USA (e-mail: fra3@cornell.edu).

F. Rana is with the School of Electrical and Computer Engineering, Cornell University, Ithaca, NY 14853 USA (e-mail: fr37@cornell.edu).

Color versions of one or more of the figures in this letter are available online at <http://ieeexplore.ieee.org>.

Digital Object Identifier 10.1109/LPT.2007.913254

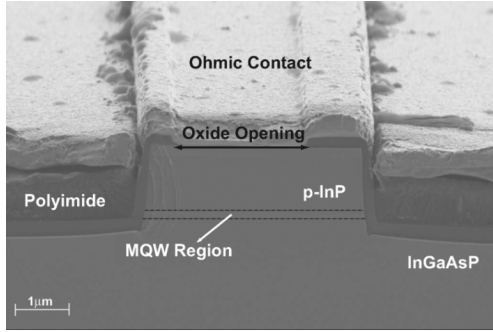


Fig. 2. Scanning electron microscope of one of the facets of the fabricated lasers. The region marked by InGaAsP is the waveguiding section which is 4 μm thick. The section marked MQW region consists of five periods of InGaAsP-based quantum wells and barriers.

E_{sat} was estimated to be approximately 27 pJ using the expression given by (1). The assumed value for the differential gain dg/dN is $7 \times 10^{-16} \text{ cm}^2$ [13].

An oxide mask was used to etch the waveguides to a depth of approximately 1.9 μm , which is 0.5 μm past the active region. The etch was performed using a $\text{Cl}_2\text{-H}_2\text{-Ar}$ -based recipe in an inductively coupled plasma etcher. After the etch, the oxide mask was removed and a 280-nm layer of oxide was deposited. A layer of thermally curable polyimide was used to planarize the waveguides (Fig. 2). The p-ohmic contacts are comprised of standard Ti-Pt-Au layers. The substrate was thinned to a thickness of 150 μm and an n-ohmic contact comprised of Ni-Ge-Au layers was evaporated. A 15- μm gap separated the gain and the saturable absorber section. By etching away the top p^+ contact layer using $\text{Cl}_2\text{-BCl}_3\text{-Ar}$ plasma etch, an electrical isolation of about 2 $k\Omega$ was achieved. The laser bars were cleaved and the facet closest to the saturable absorber segment was coated with three periods of $\text{Al}_2\text{O}_3\text{-Si}$ to achieve 90% reflectivity. The other facet was coated with a layer of Al_2O_3 to reduce the reflectivity to about 15%.

The lasers were mounted on a gold-plated copper chuck using indium solder. The temperature of the chuck was maintained at 10 $^\circ\text{C}$. The gain section was forward-biased using a dc-probe tip. To mode-lock the laser, a G-S (pitch $\approx 1.25 \text{ mm}$) high-frequency probe was used to reverse-bias the saturable absorber section via an 18-GHz bias-tee. Light from the output facet was collimated using an aspheric lens and split using a 50-50 beam-splitter cube. Light from one port of the beam-splitter was directed into an auto-correlator. Light from the other port was split again and focussed onto a high-speed 26-GHz New Focus photodiode. The electrical signal from the high-speed photodiode was monitored on an RF spectrum analyzer. The remaining light was coupled through 1-m multimode patch chord into an optical spectrum analyzer.

III. RESULTS

The total length of the first laser was 9 mm. The length of the saturable absorber section was 250 μm . With the saturable absorber initially unbiased, the laser exhibited continuous-wave (CW) lasing at a threshold current of approximately 350 mA. At a bias current of 1.6 A, the CW output power approached 280 mW. Initially, the current through the gain section was maintained at 800 mA, and the reverse bias across the saturable absorber was gradually increased. At a reverse bias voltage of

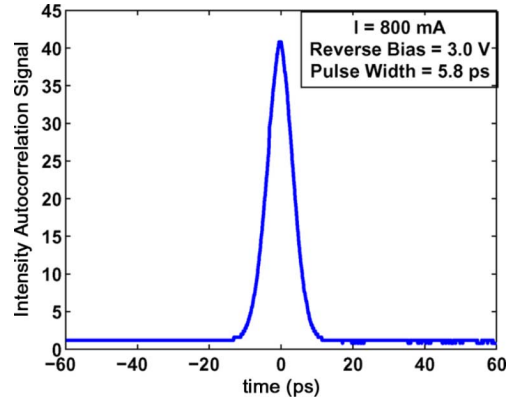


Fig. 3. Measured intensity autocorrelation of the pulse. The bias current is 800 mA and the reverse-bias voltage is -3.0 V . The pulsewidth is 5.8 ps.

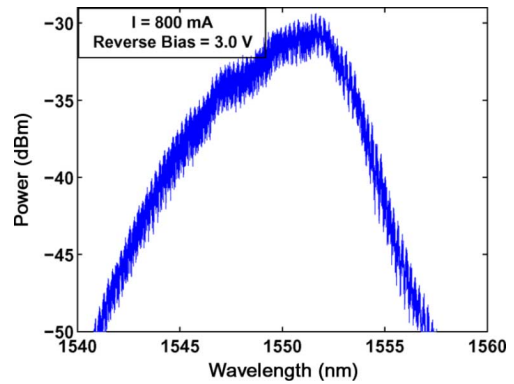


Fig. 4. Measured optical spectrum of the mode-locked pulse. The spectrum was obtained with a 10-pm resolution and, hence, the longitudinal modes of the cavity are observed.

1.4 V, the laser mode-locked. The observed pulse repetition rate was 4.6 GHz. As the reverse bias voltage was increased, the pulsewidth steadily decreased until it reached about 5.8 ps (Fig. 3). The optical spectrum for the shortest obtained pulse is shown in Fig. 4. Upon closer inspection of the spectrum, one finds that the peaks are separated by 0.037 nm corresponding to the longitudinal modes of the cavity. The reduction in the pulsewidth was also accompanied by a reduction in the average power of the laser. The reduction in pulsewidth and average power was due to the fact that the carrier sweep-out time decreases as the reverse-bias voltage is increased. This in turn increases the saturable loss in the cavity.

Mode-locking was also demonstrated for higher gain currents. In Figs. 5 and 6, the pulsewidth and the average power are shown as a function of the reverse-bias voltage across the saturable absorber section. It can be seen that for a given reverse-bias voltage, both the pulsewidth and average power increase as the gain current is raised. Furthermore, at higher gain currents, the laser mode-locks at larger reverse-bias voltages. This is due to faster carrier sweep-out time at higher reverse-bias voltages. For a gain current of 1.6 A, the laser mode-locked at a reverse-bias voltage of 1.9 V. At this point, the average power was 212 mW and the corresponding pulse energy approached 46 pJ. Although the pulsewidth at this point was around 25 ps, further increasing the reverse-bias voltage reduced the pulsewidth to just over 7 ps. The largest peak power obtained was 3.95 W at a reverse-bias voltage of 2.8 V for the

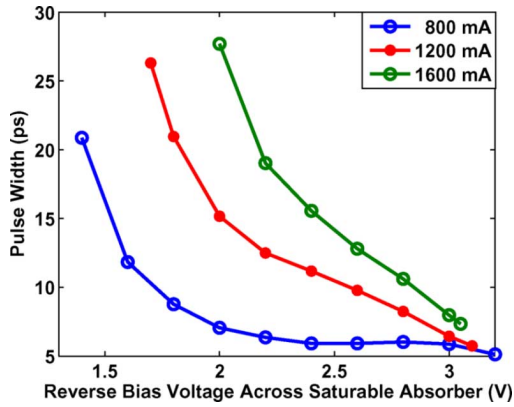


Fig. 5. Measured pulsewidth as a function of the reverse-bias voltage across the saturable absorber. The length of the laser was 9 mm.

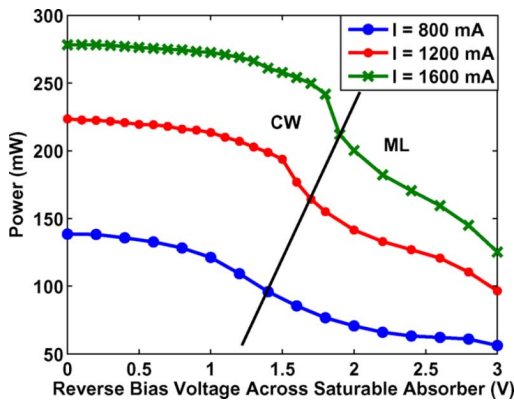


Fig. 6. Measured optical power as a function of the reverse-bias voltage across the saturable absorber for three different gain currents. CW and ML indicate the regions where the laser is operated in the continuous-wave and mode-locked regimes, respectively. The length of the laser was 9 mm.

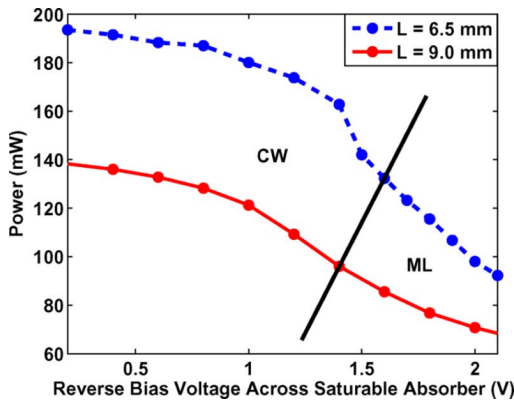


Fig. 7. Measured optical power as a function of the reverse-bias voltage across the saturable absorber for two different laser lengths (9.0 and 6.5 mm). Again CW and ML indicate the regions where the laser is operated in the continuous-wave and mode-locked regimes, respectively. The gain current for both lengths was maintained at 800 mA.

same gain current of 1.6 A. Also, the power–current efficiency at the onset of mode-locking was 133 mW/A.

Shorter lasers were found to exhibit larger power–current efficiencies. We fabricated and characterized lasers with lengths of 6.5 mm. With the saturable absorber initially unbiased, the

laser demonstrated a lasing threshold of 290 mA. To mode-lock the laser, the gain current was set at 800 mA and the reverse bias across the saturable absorber was gradually raised. The fundamental repetition rate was 6.5 GHz. The shortest pulsewidth measured was just over 6 ps. The shorter laser generated more optical power for the same gain current. In Fig. 7, the average output power as a function of the reverse-bias voltage for laser lengths of 9.0 and 6.5 mm is shown. The shorter laser has a power–current efficiency of 165 mW/A compared to 120 mW/A for the longer device right at the onset of mode-locking.

IV. CONCLUSION

We have studied passive mode-locking in high-power semiconductor lasers based on the slab-coupled optical waveguide geometry. The increased confinement factor in our devices resulted in a reduction of the threshold current by about 46% compared to the threshold current quoted for the device reported in [10]. The largest power–current efficiency recorded was 165 mW/A. Again this was a result of the increased confinement factor. Stable pulses as short as 5.8 ps have been generated directly from the laser without any external compression. The highest average power measured when the laser was mode-locked was 212 mW. The highest peak power measured was approximately 3.95 W.

REFERENCES

- [1] K. A. Williams, M. G. Thompson, and I. H. White, "Long-wavelength monolithic mode-locked diode lasers," *New J. Phys.*, vol. 6, pp. 179–179–30, 2004.
- [2] H. F. Liu, S. Arahira, T. Kunii, and Y. Ogawa, "Generation of wavelength-tunable transform-limited pulses from a monolithic passively mode-locked distributed Bragg reflector semiconductor laser," *IEEE Photon. Technol. Lett.*, vol. 7, no. 10, pp. 1139–1141, Oct. 1995.
- [3] S. Arahira, S. Sasaki, K. Tachibana, and Y. Ogawa, "All-optical 160-Gb/s clock extraction with a mode-locked laser diode module," *IEEE Photon. Technol. Lett.*, vol. 16, no. 6, pp. 1558–1560, Jun. 2004.
- [4] L. A. Jiang, E. P. Ippen, and H. Yokoyama, "Semiconductor mode-locked lasers as pulse sources for high bit rate data transmission," *J. Opt. Fiber. Commun.*, vol. 2, pp. 1–31, 2005.
- [5] F. Rana, R. J. Ram, and H. A. Haus, "Quantum noise of actively mode-locked lasers with dispersion and amplitude/phase modulation," *IEEE J. Quantum Electron.*, vol. 40, no. 1, pp. 41–56, Jan. 2004.
- [6] A. Mar, R. Helkey, T. Reynolds, J. Bowers, D. Botez, C. Zmudzinski, C. Tu, and L. Mawst, "Mode-locked multisegment resonant-optical-waveguide diode laser arrays," *IEEE Photon. Technol. Lett.*, vol. 5, no. 12, pp. 1355–1359, Dec. 1993.
- [7] A. Aschwendt, D. Lorentz, H. J. Unold, R. Paschotta, E. Gini, and U. Keller, "2.1-W picosecond passively mode-locked external-cavity semiconductor laser," *Opt. Lett.*, vol. 30, no. 3, pp. 272–274, 2005.
- [8] S. Gee, G. Alphonse, J. Connolly, and P. J. Delfyett, "High-power mode-locked external cavity semiconductor laser using inverse bow-tie semiconductor optical amplifiers," *IEEE J. Sel. Topics Quantum Electron.*, vol. 4, no. 2, pp. 209–215, Mar. 1998.
- [9] G. P. Agrawal and N. K. Dutta, *Semiconductor Lasers*, 2nd ed. New York: VNR, 1993.
- [10] J. J. Plant, J. T. Gopinath, B. Chann, D. J. Ripin, R. K. Huang, and P. W. Juodawlkis, "250 mW, 1.5 μm monolithic passively mode-locked slab-coupled optical waveguide laser," *Opt. Lett.*, vol. 31, no. 2, pp. 223–225, 2006.
- [11] J. J. Plant, P. W. Juodawlkis, R. K. Huang, J. P. Donnelly, L. J. Misagaglia, and K. G. Ray, "1.5- μm InGaAsP–InP slab-coupled optical waveguide lasers," *IEEE Photon. Technol. Lett.*, vol. 17, no. 4, pp. 735–737, Apr. 2005.
- [12] E. A. J. Marcatili, "Slab coupled waveguides," *Bell Syst. Tech. J.*, vol. 53, no. 4, pp. 645–674, Apr. 1974.
- [13] S. Seki, T. Yamanaka, W. Lui, and K. Yokoyama, "Theoretical analysis of differential gain of 1.55 μm InGaAsP/InP compressive-strained multiple-quantum-well lasers," *J. Appl. Phys.*, vol. 75, pp. 1299–1303, 1994.